https://dx.doi.org/10.21577/0103-5053.20230045

*J. Braz. Chem. Soc.*, Vol. 34, No. 9, 1333-1346, 2023


Article

# Controlled Release of Rutin from Babassu Coconut Mesocarp Starch Films

*Liane M. Carvalho,[a] Cicero W. B. Bezerra,[a] Claudia Q. da Rocha,[b] Letícia N. de Oliveira,[a] Luna N. Vasconcelos[b] and Sirlane A. A. Santana[*,a]*

[a]*Laboratório de Química de Interfaces e Materiais, Departamento de Química, Universidade Federal do Maranhão, Avenida do Portugueses, 1966, Cidade Universitária, 65080-805 São Luís-MA, Brazil*

[b]*Laboratório de Química de Produtos Naturais, Departamento de Química, Universidade Federal do Maranhão, Avenida do Portugueses, 1966, Cidade Universitária, 65080-805 São Luís-MA, Brazil*

Rutin is found in several plant sources and has therapeutic effects with excellent healing potential. Its use is restricted due to its low aqueous solubility, requiring a carrier matrix that allows an adequate delivery system. Biopolymer matrices can release the active ingredient in a controlled manner, keeping it within the therapeutic range and minimizing side effects. This study used babassu mesocarp starch films prepared by different routes as *Arrabidaea brachypoda* DC Bureau (AB) leaf extract carrier matrices to produce a controlled release system. The films were produced by the casting method, and the AB extract was incorporated in the proportion of 0.5% m/m of dry starch. The presence of the extract in the matrix was identified with Fourier transform infrared spectroscopy (FTIR) and X-ray diffractometry (XRD) data and functional analyses. The *in vitro* release of the AB extract was carried out in phosphate-buffered saline, pH 7.4, and adapted to the Korsmeyer-Peppas model, with coefficients of determination ($R^2$) ≥ 0.9018. The release exponents (n) revealed that the release mechanism is diffusion controlled. Different kinetic constant values (k) indicated that the treatments employed allowed slower and more controlled release profiles, according to the route chosen for matrix preparation. Thus, the materials produced emerge as a new approach to releasing vegetable extracts.

**Keywords:** controlled release, vegetable extracts, biopolymeric films, babassu mesocarp

## Introduction

Rutin (Figure 1), a glycoside flavonoid composed of a quercetin molecule linked to glucose and rhamnose molecules,[1] presents several beneficial therapeutic effects, such as anti-allergic, cytoprotective, anti-tumor, anti-inflammatory, antibacterial, antiviral, and anti-fungal properties.[2-4] Moreover, rutin has free radical scavenging effects on oxidizing species, such as the superoxide radical, which gives it great potential for healing purposes.[1,3] However, its pharmaceutical use is restricted due to its low solubility in water, which hinders direct oral administration.[4-6] Low solubility, combined with low oral bioavailability, limits its potential as a therapeutic agent or, at the very least, potential routes of administration.[4,7]

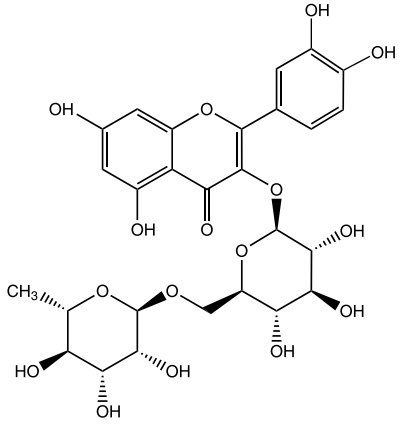


**Figure 1.** Chemical structure of the rutin flavonoid.

It can be found in plant extracts of the genus *Arrabidaea*, mainly in the extract of the leaves of the species *Arrabidaea brachypoda* (DC) Bureau, a plant with known pharmacological activity.[8] Different extracts obtained

*e-mail: saa.santana@ufma.br
Editor handled this article: Fernando C. Giacomelli (Associate)

from its leaves, roots, and stem have anti-fungal effects,[9] anti-inflammatory and antinociceptive effects,[10,11] besides action on *Trypanosoma cruzi in vitro* and *in vivo*,[12] and gastroprotective effects *in vivo*.[13]

The study of plant species with potential pharmacological capabilities has drawn much attention.[14,15] Extracts obtained from medicinal plants preserve their various active components, such as alkaloids, tannins, flavonoids, and saponins, which have high pharmacological power,[8,14] and have been applied in the development of new phytomedicines. Extracts are preferable because plant materials contain a wide range of compounds that work synergistically or individually to provide therapeutic effects and are generally cheaper and more accessible than synthetic drugs.[15-18] It is necessary to use carrier matrices that guarantee its integrity to preserve the properties of the extract. Releasing the active ingredients in a controlled way increases their bioavailability and ensures therapeutic effects.[15,17]

Matrices of biopolymer origin are relevant due to their biocompatibility, availability, non-toxic, biodegradability, and low cost.[19-21] In addition, they can stabilize the release of the active ingredient. Systems that can modulate the release favor more selective and long-term actions, keeping the product in the therapeutic range for an adequate time, contributing to its efficiency, and minimizing possible side effects.[19,22-25]

Among the polymers used in the preparation of drug carriers, we highlight cellulose derivatives,[26-28] chitosan,[29,30] alginate,[31,32] gelatin,[33,34] polylactic acid,[35,36] poly(lactic-*co*-glycolic acid),[37] polyhydroxyalkanoates[38] and starch.[39,40] They can be applied in the form of powder, microspheres, and films, these being an alternative to conventional oral delivery, possessing the advantage of making the treatment more comfortable and functional, and can be administered topically.[41,42]

Starch is an important biopolymer of plant origin with good film-forming ability, composed mainly of two polysaccharides: amylose and amylopectin, consisting of α-D-glucose units linked by α-1,4 and α-1,6 glycosidic bonds. Amylopectin is extensively branched and represents 70-80% of starch.[39,43-45] The amylose content varies from 15 to 30%, depending on the origin of the starch, and is responsible for the formation of stable and resistant hydrogels and films.[46,47] It is classified according to its crystallinity into type A, B, or C starch.[48] Moreover, it has been employed in film form as a carrier matrix for drugs and plant extract.[17,39,41,49-52]

The babassu coconut (*Orbignya pharelata* Mart.) is a valuable natural resource in the North and Northeast regions of Brazil, widely used for the production of vegetable oil. It has four main parts, schematized in Figure 2. They are epicarp, mesocarp, endocarp and the almonds, from which the oils are extracted.

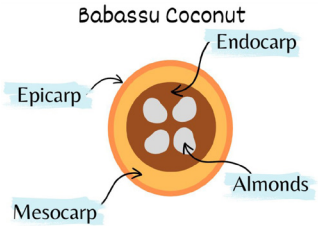


**Figure 2.** Schematic representation of the cross-section of babassu coconut and its parts: epicarp, mesocarp, endocarp and the almonds.

Babassu mesocarp, considered as an input from the exploitation of babassu coconut is commonly consumed as flour in human and animal food, and used in popular medicine, for healing and anti-inflammatory purposes.[53-56] It contains, in its composition, about 50 to 70% starch with high amylose content, which indicates its potential for film formation. Babassu mesocarp can be an exciting choice for a starch raw material in formulations of films carrying active substances, due to its chemical composition.[22,44,57]

In this work, we innovate by producing films of babassu mesocarp as carrier matrix of the hydroethanolic extract of the leaves of *Arrabidaea brachypoda* DC Bureau, rich in rutin, called AB. As far as we know, there are no reports in the literature that aim to evaluate its capacity of controlled release for future topical applications, especially for healing purposes.

## Experimental

### Materials

Babassu mesocarp (BM) was purchased from local businesses, and ground and sieved to the particle size range between 88 and 177 μm. Phosphate-buffered saline (PBS) 0.1 mol $L^{-1}$ was prepared employing $Na_2HPO_4$ and $KH_2PO_4$ from Synth (São Paulo, Brazil), and HCl from Isofar (Rio de Janeiro, Brazil) 0.1 mol $L^{-1}$ was used for pH adjustment. *Arrabidaea brachypoda* DC Bureau (AB) extract was obtained from dried leaves. For the controlled release assay, rutin (RT) was used as a reference standard, supplied by the company Fagron Brasil LTDA (São Paulo, Brazil), with 70% purity. All other chemical reagents used in this study were of analytical grade, used as received and without further purification.

### Purification of babassu mesocarp (BM)

The purification of BM was performed at different pHs, aiming to remove possible impurities present in

the raw material. Based on the method described by Maniglia *et al*.,[44] BM was immersed in distilled water, pH 6.5 (NT), 0.25% NaOH solution, pH 10 (BT), and 1% ascorbic acid solution, pH 3 (AT), in a ratio 1:2. After 16 h, the mixture was ground and the material was sieved on 80, 200, and 270 mesh sieves. The retained product was ground and sieved four times again. The resulting material was vacuum filtered, and the supernatant was discarded. The starch obtained was again solubilized in water until the supernatant reached a constant pH. The solid was then dried in an oven at 45 °C for 12 h, ground, and sieved at 80 mesh.

### Preparation and chromatographic profile of the leaf extract of *Arrabidaea brachypoda* D.C Bureau

The extract of the dried leaves of *A. brachypoda* was obtained by maceration at room temperature, by exhaustive percolation with EtOH:$H_2O$ solution (7:3 v $v^{-1}$). The crude hydroethanolic extract was obtained after filtration and concentration in a rotary evaporator under vacuum at 40 ºC, and then lyophilized and coded in this work as AB. The flavonoid identification was made by high-performance liquid chromatography (HPLC). 30 mg of the sample went through the clean-up process with PhenomenexStrata C18 cartridges (SPE), previously activated and equilibrated with 2 mL of MeOH:$H_2O$ (9:1) solution. After the evaporation of the solvent, 10 mg of the sample were solubilized in 2 mL of MeOH: $H_2O$ (9:1) solution, and then 10 µL were injected into a Shimadzu HPLC/UV/Vis (Kyoto, Japan), consisting of a solvent supply module with a double piston pump, with UV detector SPA-10A. The RP C18 100°A (150 × 4.8 mm) column was used, with a flow rate of 1 mL $min^{-1}$, and gradient evolution from 5 to 100% of B in 70 min, using as solvents A: $H_2O$ + 0.01% formic acid and B: MeOH + 0.01% formic acid. The data were collected at 254 nm and processed using Shimadzu LC Solution v.4.0 software.

### Film preparation

Films were produced by casting method.[44,58,59] A suspension of the amylaceous solids, 3% (m/m) in distilled water, was homogenized in a magnetic stirrer for 30 min, then heated to 80 ± 1 ºC, under constant stirring, for another 30 min. The glycerol plasticizer was added (20 g glycerol/100 g starch) and the mixture was heated for another 15 min. Subsequently, the solution was poured onto 12 cm diameter polystyrene plates, maintaining a standard of 25 g. The material was dried in an oven at 45 ºC for 24 h, detached from the surface, and stored in a desiccator.

### Incorporation of AB extract into biopolymer matrices

0.015 g of the AB extract solubilized in 2 mL of methanol was added to the 3% (m/m) mesocarp suspension in distilled water and the films were prepared following the methodology described in the "Film preparation" sub-section. The new films were named BM-AB, NT-AB, BT-AB, and AT-AB. Table 1 summarizes the nomenclature of all samples.

**Table 1.** Description of the acronyms used in each sample and the routes employed

| Sample code | Description of the sample | Route |
|---|---|---|
| BM | babassu mesocarp powder and film | *in natura* |
| BT | starch powder and film without extract | basic route pH 10 |
| AT | | acid route pH 3 |
| NT | | neutral route pH 6.5 |
| BM-AB | film carrier with *Arrabidaea brachypoda* leaves extract | babassu mesocarp *in natura* + 0.015 g AB |
| BT-AB | | starch obtained for basic route + 0.015 g AB |
| AT-AB | | starch obtained for acid route + 0.015 g AB |
| NT-AB | | starch obtained for neutral route + 0.015 g AB |

BM: babassu mesocarp; AB: *Arrabidaea brachypoda* DC Bureau.

### Characterization

#### Fourier transform infrared spectroscopy (FTIR)

FTIR of films and pure polymers were recorded in a Shimadzu spectrophotometer, (model IR Prestige-21, Kyoto, Japan), in the range of 4000 to 400 $cm^{-1}$, in 60 scans and resolution of 4 $cm^{-1}$. Only the pure polymers were analyzed in powder form on KBr tablets. Film samples were applied directly to the support of the equipment and analyzed in the mentioned range.

FTIR of AB extract and RT were also recorded in the same conditions, in powder form, on KBr tablets.

#### X-ray diffraction (XRD)

X-ray diffraction measurements were performed in a Bruker D8 Advance diffractometer (Billerica, USA), with a Cu Kα radiation tube (λ = 0.15418 nm) operating at 40 kV, 40 mA, with angle 2θ ranging from 3 to 70°, and scanning amplitude equal to 2θ *per* min (0.04º $s^{-1}$). The crystallinity indexes (CrI) were quantitatively estimated as the ratio between the areas of the major ($I_o$) and minor ($I_{am}$) peaks found in the XRD data, according to equation 1:

$$CrI(\%) = 100 \times (I_o - I_{am})/I_o \quad (1)$$

### Scanning electron microscopy (SEM)

Micrographs (SEM) of the starches were obtained on a FEI TECNAI G$^2$ F20 microscope (Eindhoven, The Netherlands) operating at 200 kV. The samples were prepared by depositing small amounts of the powders directly onto carbon strips under metal support, fixated with nitrogen.

### Moisture content (ω)

The moisture content of the film (ω) was determined with a few modifications based on AOAC standard 930.04.[60] Proof cuts of 2.5 × 2.5 cm were initially weighed and equilibrated in environments at 58% relative humidity (RH, saturated NaBr solution) and 75% RH (saturated $Na_2SO_4$ solution) at 25 ºC for 24 h. They were subsequently dried in an oven at 105 ºC for 12 h. The calculation of ω was performed according to equation 2.

$$\omega(\%) = [(m_i - m_f)/m_i] \times 100 \quad (2)$$

where $m_i$ is the total initial mass of the film sample (g); $m_f$ is the dry mass of the film (g).

### Water solubility (S)

The water solubility of films (S) was based on the methodology described by Suh *et al.*[46] applying equation 3. The dry films, cut in the size of 2.5 × 2.5 cm, were weighed ($p_i$), immersed in 50 mL of distilled water, and kept under stirring (100 rpm) at 25 ºC for 24 h. After this period, the samples were removed from the water and dried in an oven at 105 ºC for 12 h to determine the final dry weight, $p_f$, of the material that was not solubilized.

$$S(\%) = [(p_i - p_f)/p_i] \times 100 \quad (3)$$

where $p_i$ is the mass of the dry film (g) and $p_f$ represents the final mass of the film (g) after solubilization and drying.

### Absorption capability in aqueous solutions

The absorption capability of the films was evaluated in deionized water, saline solution (NaCl 0.9% m v$^{-1}$), simulated body fluid (SBF), prepared according to Kokubo *et al.*,[61] and PBS. 2.5 × 2.5 cm film samples were immersed in 20 mL of the referred solutions at 37 °C for 24 h. After this period, the excess solvent was removed lightly with a paper towel for about 5 s, and the final mass was immediately determined on an analytical balance. The maximum absorption capacity ($Abs_{max}$) was calculated according to equation 4:

$$Abs_{max} = (m_u - m_s)/m_s \quad (4)$$

where $m_u$ represents the mass of the film while wet, and $m_s$ represents the mass of the dry film.

### Mechanical properties

Elongation at break (ε), tensile strength (TS), and Young's modulus (E) were determined according to ASTM D882-18,[62] in a Biopdi universal testing machine, model MBIO II (São Paulo, Brazil). Specimens with 8.0 cm length and 2.5 cm width were fixed on the equipment's claws (initial claw spacing of 50 mm on average), with speed fixed at 20 mm min$^{-1}$. The mechanical properties experiments were performed in triplicate for each sample. The TS given in MPa and ε given in percentage were calculated by equations 5 and 6, respectively.

$$TS(\%) = MF/A \quad (5)$$

$$\varepsilon(\%) = (\Delta l/l_0) \times 100 \quad (6)$$

where MF is the maximum force at the moment of break; A is the cross-sectional area of the film, Δl is the final distance of the separation of the claws; $l_0$ is the initial separating gap between the equipment's claws.

Young's modulus was determined by equation 7, where TS is the tensile strength obtained by equation 5, and ε is the longitudinal elastic deformation.

$$E = TS/\varepsilon \quad (7)$$

### *In vitro* release of AB extract

The release assay was based on the methodology cited in the literature[63,64] with some adaptations. Films measuring 5 × 5 cm, while in contact with 50 mL of PBS solution at a temperature of 37 ºC, were kept under constant stirring at 100 rpm for up to 48 h and, at pre-defined time intervals, aliquots of 2 mL of the solution were removed, and the amount of extract released was quantified. With each aliquot removed, an equal volume of fresh PBS solution (pH 7.4) was added to the medium to keep the initial volume of the assay constant. The amount of extract released was determined by the colorimetric method of complexation with 2% m/v methanolic solution of $AlCl_3$[65] from an external calibration curve of rutin, constructed in triplicate, in the concentration range of 5 to 35 mg L$^{-1}$, in a KASUAKI UV-Vis spectrophotometer (Tokyo, Japan), model IL-592-BI. The *in vitro* release experiments were performed in triplicate for each sample.

The release mechanism of the extract was evaluated by fitting the Korsmeyer-Peppas model (equation 8) to the data obtained.

$$M_t/M_\infty = kt^n \quad (8)$$

where $M_t$ and $M_\infty$ are the absolute cumulative amount of drug released at t time and infinite time, respectively; k is the kinetic constant, and n is the release exponent indicating the release mechanism.

### Statistical analysis

All experiments were performed in triplicate, and the data were expressed as mean ± standard deviation (SD). The data were submitted for analysis of variance (ANOVA). Tukey's multiple comparison test with a $P$ value ≤ 0.05 was applied to determine significant differences.

## Results and Discussion

### Characterization of polymers by FTIR spectroscopy and XRD

FTIR spectroscopy was used to evaluate the starches before and after the applied treatments. The spectra of the samples BM, BT, AT, and NT (Figure 3a) showed the characteristic peaks of starch materials. At 2915 $cm^{-1}$, a characteristic band of elongation of the C–H and $CH_2$ bonds is observed.[45] The vibrational transition at 1623 $cm^{-1}$ is attributed to vibrations of adsorbed water molecules on the amorphous regions of the material.[66] In starch spectra, some bands between 950 and 1200 $cm^{-1}$ are commonly observed due to the stretching of the C–O bonds of the carbohydrates.[45] The bands at 841-739 $cm^{-1}$ can be attributed to the =C–H deformations of monosubstituted aromatic rings.[67] Maniglia and Tápia-Blácido[45] and Vieira *et al.*[66,67] also characterized the babassu mesocarp in their work, obtaining results similar to those found in this work.

The band at 1159 $cm^{-1}$ is attributed to the α 1-4 C–O–C bond[66] referring to the starch and appears with little intensity only in BM and NT, being absent or undetectable in AT and BT, probably due to the limitations of the measuring apparatus itself.

An X-ray diffractometer was used to determine the variation in crystallinity, to understand better the impact of

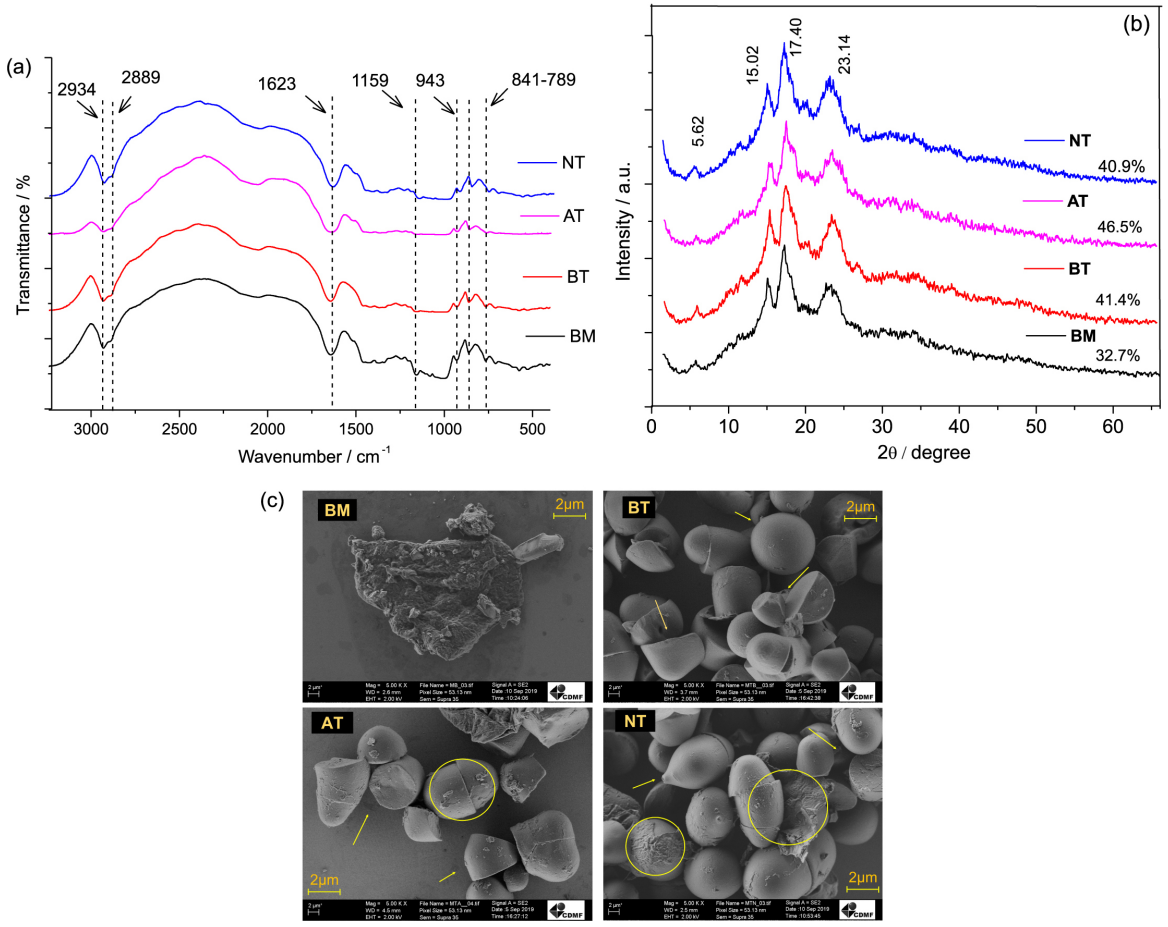


**Figure 3.** (a) FTIR (KBr) spectra of babassu mesocarp (BM) *in natura* and of the starches extracted by basic (BT), acid (AT), and neutral (NT) routes. (b) X-ray diffraction patterns of babassu mesocarp (BM) *in natura* and of the starches extracted by the basic (BT), acid (AT), and neutral (NT) routes. (c) Morphology of starch granules from babassu mesocarp (BM) *in natura*, and by the basic (BT), acid (AT), and neutral (NT) routes.

the treatments employed on the crystalline and amorphous regions of the starch granules. As illustrated in Figure 3b, it is observed that the same characteristic diffraction peaks were maintained for all materials. Peaks near 5, 17, and 22° are characteristic of type B starch,[68] typically found in tubers. Peaks near 15° are characteristic of type A starch,[68] usually found in cereals. Therefore, the materials presented characteristics of a mixture of type A and B starch, referred to as type C starch.[45,68] The intensity of the peak near 20° is indicative of the presence of amylose-lipid complexes, and its intensity is relative to the amylose content,[69] and this peak was identified in the four studied samples. The degree of starch crystallinity calculated by XRD varies from 15 to 45% and is mainly related to this structure.[57] The crystalline region of the starch granule is constituted by the double helices of parallel chains of amylopectin, and by the linear structures of amylose, tending to be more compact.

In contrast, the less ordered amorphous region contains the branching points of the side chains of amylopectin and possibly some amylose.[70] Starches with higher amounts of amylose form films with better properties. The treatments influenced the purified starches' degree of crystallinity, calculated according to equation 1. AT had the highest crystallinity index (46.5%), probably due to the higher amylose content in relation to the others, while BT and NT presented a degree of crystallinity of 41.4 and 40.9%, respectively. There was an increase in crystallinity when compared to BM with 32.7% in all cases. Maniglia *et al.*[44] also found that after the purification of babassu mesocarp by acid, basic and neutral treatment, there was an increase in crystallinity, suggesting that the routes used in the purification process, removed impurities, and consequently, the materials had higher starch content.[71]

Figure 3c shows the scanning electron micrographs for the starches extracted by the basic, acid, and neutral routes, compared to the mesocarp *in natura*. BT, AT, and NT granules showed oval geometry with some broken granules of semi-spherical shape and residues adhered to the surface, more evident in AT and NT (circles). Similar results were reported by Maniglia and Tápia-Blácido,[45] who attributed the surface defects of starch granules to the purification process, which involves agitation, filtration, grinding, and drying, thus affecting the quality and surface strength of the granules. This procedure allows the granules to absorb water and swell irreversibly. Thus, the long chains of amylose are broken and move easily from the interior to the surface, causing various defects, such as rupture and adhesions on the surface of the granules.[57]

Compared to BM, the granules of starches obtained by the chosen routes presented a smooth surface with oval and polygonal geometry (arrows). Granules with polygonal geometry are susceptible to higher water absorption, and greater power of expansion and smooth surfaces are adequate when starches are used to prepare smooth and homogeneous polymeric films.[57]

## Characterization of the crude extract of the leaves of *Arrabidaea brachypoda* D.C Bureau (AB)

Before the incorporation process of the AB extract in the films, it was characterized by HPLC and FTIR. In Figure 4a, the AB extract presented rutin, a glycosylated flavonoid abundantly found in several natural sources, as a significant component and it was identified by comparison with the standard, showing the same retention time at 28 min. The extract is well known and has been characterized and studied for various purposes.[11-13,72,73]

Figure 4b shows the infrared spectrum as an auxiliary characterization in the comparison of the AB extract and rutin, used as the reference standard in this study. A remarkable similarity was observed between both. By analyzing the spectrum of the standard rutin (RT), one notices the band at 3333 $cm^{-1}$ attributed to the stretching of the phenolic hydroxyl. The aromatic axial deformation of the C–H bond is observed at 2930 $cm^{-1}$. The band at 1667 $cm^{-1}$ is assigned to the carbonyl stretching vibration

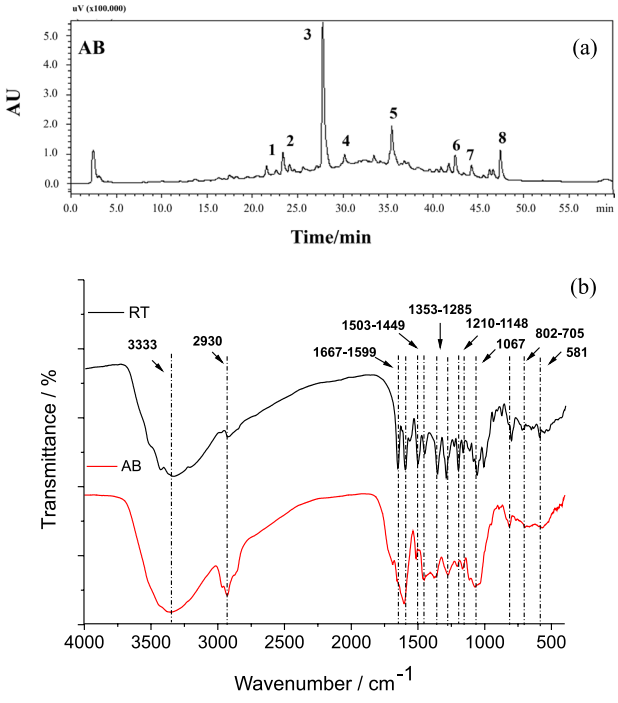


**Figure 4.** (a) HPLC/UV-Vis chromatogram of the hydroethanolic extract of *Arrabidaea brachypoda* leaves. Analysis conditions: column C18 100 A (150 µm × 4.6 µm), eluents: A (water + formic acid) and B (methanol), gradient 5 to 100% of B in 70 min. Flow rate: 1 mL $min^{-1}$. (b) FTIR (KBr) of the crude extract of *A. brachypoda* leaves (AB) compared with the rutin standard (RT).

band (C=O), the bands at 1599, 1503, and 1449 $cm^{-1}$ correspond to the stretching of the phenyl ring (C=C). The band at 1353-1285 $cm^{-1}$ is assigned to the stretching of –C–CO–C– bonds and the one at 1067 $cm^{-1}$ is attributed to stretching vibrations of the C–O group in alcohols and phenols. The bands at 1210 and 1148 $cm^{-1}$ correspond to the stretching of C–O–C and deformation of the glycosidic units O–H groups. The band at 802 $cm^{-1}$ corresponds to the out-of-plane vibration of $R_2C$=CHR bonds. At 705 $cm^{-1}$ there are the angular deformations of monosubstituted aromatic rings, and at 581 $cm^{-1}$ there is the characteristic band of CH=CH out-of-plane deformations.[74] Hooresfand *et al.*[75] also observed characteristic peaks in the FTIR, related to specific bands of rutin, as reported in this work.

Comparing the FTIR of RT and the AB extract, there are similarities between the peaks, which proves the presence of rutin in most of the extract, therefore, used as a biochemical marker of it.

## Characterization of films loaded with AB extract

### FTIR spectroscopy

The most significant bands of the films are presented in Figure 5. At 1653 $cm^{-1}$, a band is attributed to the OH group's axial deformation with higher intensity than Figure 3a, originating from adsorbed water. This occurs due to the addition of glycerol, which contributes to the retention of water molecules on the film surface. The bands at 1250 and 941$cm^{-1}$ are assigned to the stretching of C–O bonds. The bands at 869 and 762 $cm^{-1}$ refer to out-of-plane vibrations of the =C–CH bonds. The films presented the same bands observed in the precursor starches (Figure 3a).

In the infrared spectrum of the films after the incorporation of AB extract (BM-AB, BT-AB, AT-AB and NT-AB) one may notice the set of bands reported in the films before the incorporation of extract, with the addition of two more evident bands comprised within the region of 584-520 $cm^{-1}$, which are related to the CH=CH out-of-plane group deformations. This band was not observed in the precursor starches and is present in the spectrum of the AB extract, indicating that the extract is indeed present in the films.

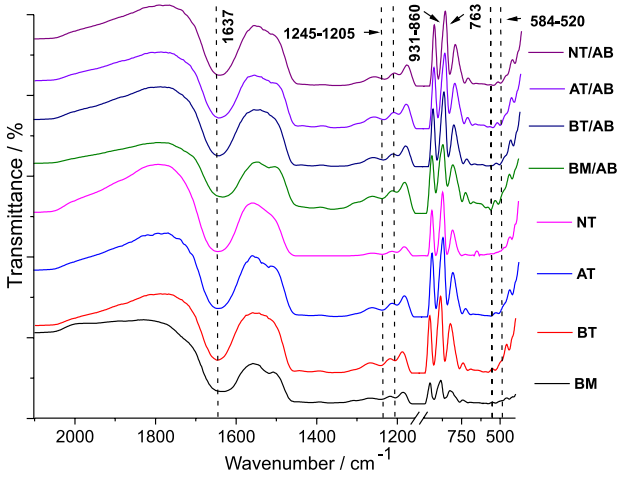


**Figure 5.** FTIR (KBr) spectra of the films before (BM, BT, AT, N T) and after (BM-AB, BT-AB, AT-AB, NT-AB) the incorporation of the extract.

### Film analysis by X-ray diffraction

The films of the extracted starches (Figure 6) maintained the diffraction profile evidenced in Figure 3b, showing peaks at angles close to 5, 15, 17, and 20º. However, a new peak can be observed at 19.82º, justified by the gelatinization and retrogradation processes. The starch molecules tend to rearrange themselves in a more organized way, favoring the increase of crystallinity, and consequently, better defining the diffraction patterns. Similar behavior was related for Maniglia *et al.*[44]

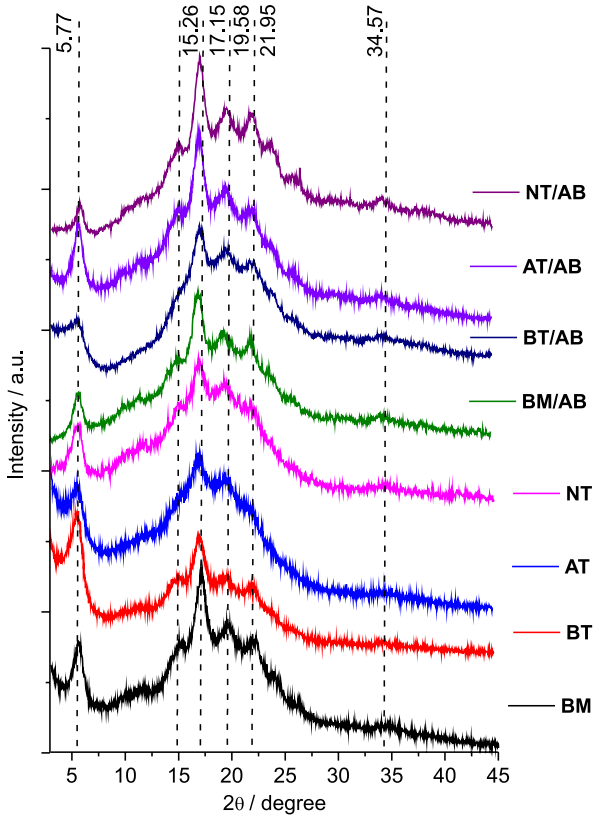


**Figure 6.** X-ray diffraction patterns of the films before (BM, BT, AT, NT) and after (BM-AB, BT-AB, AT-AB, NT-AB) the incorporation of the extract.

Analyzing the films after the incorporation of the extract, one notices sharper peaks at 21.91 and 34.57º in the diffraction patterns of all films. They are associated with AB extract incorporated into the films. In the gelatinization

process, the starch granules tend to swell, as it has two basic units, amylose, and amylopectin, the second one being branched, and, when swelling, the water molecules tend to lodge between these units, forming a gelatinous material.[76] In the cooling phase, and above the glass transition phase, amylopectin, and amylose present high molecular mobility, facilitating the organization and intermolecular hydrogen bonding between the chains to a semi-crystalline state, called retrogradation. During retrogradation, the branched structure of amylopectin reorganizes at a lower rate than linear amylose. This process is responsible for the crystallinity of the film.[76]

In the extract incorporation process, apart from water molecules, the AB extract may also be interacting with amylose and amylopectin molecules, thus changing the crystallinity of the films. The difference between the samples supports the fact that the extract was incorporated into the film.

### Moisture, absorption capacity in aqueous solutions and solubility

To identify the functional characteristics of the produced films, the variation in responses before and after incorporation of the extract at different relative humidities (ω) was evaluated. When equilibrated at RH 58%, the data indicated that these presented ω values close to each other, with contents varying between 10 and 12% (Figure 7a). It is observed that, in this case, the insertion of the extract caused a significant difference only in the BT-AB film.

Comparing the group of films without extract, BT and NT varied significantly. The relative humidity was increased to 75% to evaluate the films under extreme conditions (Figure 7b). When equilibrated in this environment, the humidity values varied between 9 and 14%. In this environment, among the films without extract (BM, BT, AT, and NT) the only one that varied significantly was the AT film. On the other hand, films with incorporated extract (BM-AB, BT-AB, AT-AB, and NT-AB) kept the same profile, with values very close to those obtained at RH 58%. Evaluating the significant differences, the films showed similar behavior, except for AT.

Moisture is an important parameter and is linked to stability in relation to the type of film application. Films for topical use should be able to retain and transport moisture at appropriate levels to avoid drying or maceration of the wound due to accumulation of fluid. In starch-rich films, this can be justified based on its amylose and amylopectin contents. The free hydroxyls in the amylose form a network of rigid strands, and the pores present in this network can retain higher water vapor content,[46] for this reason, it is expected that in higher RH environments, the moisture of the films is higher. At RH 75%, the matrices with extract presented constant ω values, which means that the extract interacts with the free hydroxyls of the matrix starch, and for this reason, the water vapor uptake is hindered.[77,78] This is a beneficial characteristic for topical use films because, in a possible lacerated environment, the film should have the ability to promote an environment with constant humidity and contribute to the cell regeneration process.[79,80]

Similar results were reported by Devi and Dutta,[81] as in their work they developed nanocomposite films of starch/chitosan/hallosyte for application in topical dressings.

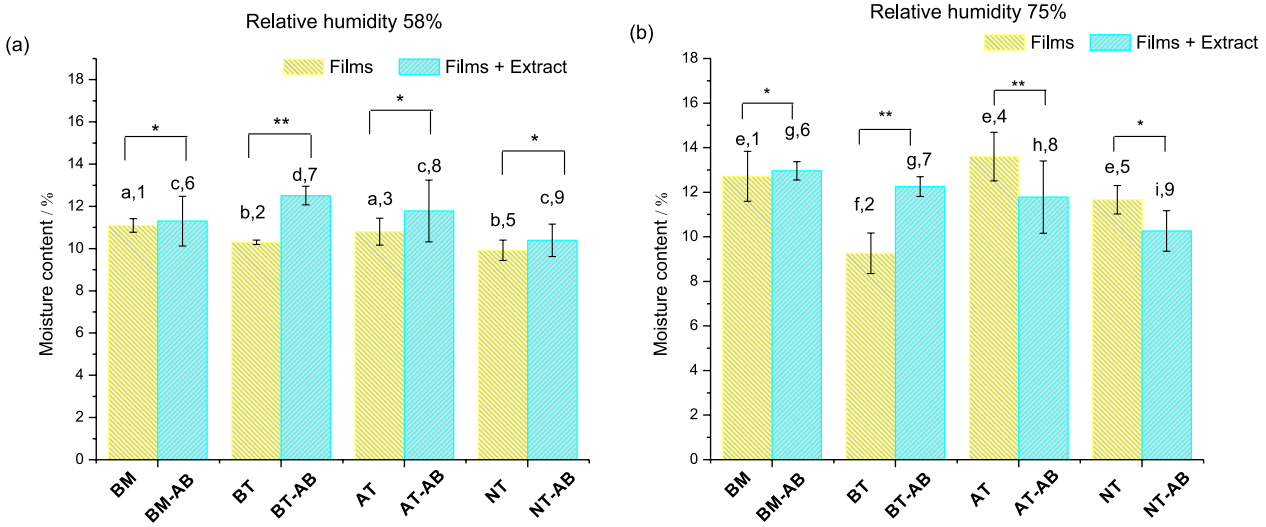


**Figure 7.** Relative humidity (%) of balanced films in environments with (a) RH 58% (NaBr saturated) and (b) RH 75% ($Na_2SO_4$ saturated). Equal letters in the same color indicate no statistically significant difference ($p \leq 0.05$) by the Tukey's test. Different numbers in the same color in the two environments indicate a statistically significant difference ($p \leq 0.05$) by the Tukey's test between the samples. (*) Indicates no significant difference between a pair of samples, (**) indicates a significant difference between a pair of samples.

The material produced showed good moisture retention capacity, being promising for healing processes.

Data regarding the maximum absorption capacities in PBS, SBF, and 0.9% NaCl solutions (Table 2) showed that the precursor films, when compared among themselves, were statistically similar in PBS, except for AT, which varied within the group. There was no significant difference between the group of films with extract, but when compared to the precursors, all of them varied significantly. In BFS, the same behavior within the film group before and after incorporation of the extract, observed in PBS, is noticed. When the films were compared before and after incorporation, significant differences were observed for BM/BM-AB, AT/AT-AB, and NT/NT-AB. As for NaCl, within the group of films before the incorporation of the extract, all varied significantly and, after incorporation, only AT-AB had significant variation.

Comparing the pairs of samples (before and after incorporation), significant variation was observed for all cases. As for solubility, it was observed that the matrices present excellent stability in aqueous media, keeping themselves intact, with a solubilization percentage between 4.19 and 8.44%. These characteristics must be evaluated for topical application films, as the membrane must maintain its integrity for a suitable period of time, in order to release the active principle without immediately losing its integrity.

The ions in the fluids can induce the shielding of remaining free charges in polysaccharides, reducing the electrostatic repulsion between the polymer chains, resulting in a compacted and less hydrophilic structure with lower liquid absorption capacity.[82] The presence of a greater number of simple bonding –OH groups on the surface of films from starch, and their availability to make hydrogen bonds with water, seem to positively affect both their ability to absorb moisture and solubility.[17]

For this reason, when comparing the fluid absorption values between the matrices, it is noted that the films without extract have slightly higher absorption capacities. The decrease in absorption values in films with extract can be explained by the interference between the polymers and the extract, leading to less expandable networks and lower solvent capture capacity.[17] This is an important matter, because the availability of free –OH groups facilitates the diffusion of water molecules in the film, causing it to swell and break, leading to the natural loss of mass and, consequently, when discussing matrices carrying active substances, this process would more easily release the active ingredient.[83] Due to the stability of the membranes regarding solubility and fluid absorption, it can be inferred that the matrices produced can be promising in controlled release systems.

Similar results were reported by Costa *et al.*,[17] when producing starch films containing pomegranate peel for use as a dressing, they observed that the films containing the active principle formed less expandable networks and with less ability to solubilize and capture solvents, favoring the integrity of the matrix during solubility and swelling tests in different solvents. Therefore, they are promising for this application. It is worth noting that after the incorporation of the extract, the films maintained the same profile, which suggests that the stability does not decrease after the addition of the extract, this means that the produced film is promising in applications that require more stable materials, for example, a dressing which needs to stay in contact with the surface for a long period of time.

## Mechanical properties

The mechanical properties of the films before and after incorporation of the extract are shown in Figure 8. It

**Table 2.** Liquid uptake (PBS buffer, SBF and 0.9% NaCl) and solubility (S) of different starch isolated for different routes with and without extract addiction

| Sample | PBS | SBF | NaCl 0.9% | S / % |
|---|---|---|---|---|
| | Absorption$_{max}$ 37 °C / (g g$^{-1}$) | | | |
| BM | 1.43 ± 0.19$^{a,A}$ | 1.42 ± 0.26$^{a,A}$ | 1.28 ± 0.01$^{a,A}$ | 8.44 ± 1.44$^{a,A}$ |
| BT | 1.76 ± 0.48$^{b,C}$ | 1.26 ± 0.13$^{a,C}$ | 1.46 ± 0.02$^{bC}$ | 4.19 ± 1.51$^{b,B}$ |
| AT | 1.62 ± 0.01$^{a,E}$ | 1.99 ± 0.26$^{b,D}$ | 2.15 ± 0.08$^{c,E}$ | 5.18 ± 0.33$^{c,D}$ |
| NT | 1.77 ± 0.15$^{a,G}$ | 1.69 ± 0.09$^{a,F}$ | 1.62 ± 0.04$^{d,G}$ | 7.45 ± 0.86$^{a,D}$ |
| BM-AB | 1.04 ± 0.01$^{c,B}$ | 1.06 ± 0.02$^{c,B}$ | 1.11 ± 0.04$^{e,B}$ | 6.01 ± 1.74$^{d,A}$ |
| BT-AB | 1.06 ± 0.08$^{c,D}$ | 0.92 ± 0.04$^{c,C}$ | 1.21 ± 0.03$^{e,D}$ | 8.36 ± 0.10$^{d,C}$ |
| AT-AB | 1.22 ± 0.01$^{c,F}$ | 1.34 ± 0.20$^{c,E}$ | 1.49 ± 0.17$^{f,F}$ | 5.68 ± 1.47$^{d,D}$ |
| NT-AB | 1.03 ± 0.02$^{c,H}$ | 1.04 ± 0.02$^{c,G}$ | 0.99 ± 0.05$^{e,H}$ | 5.75 ± 0.28$^{d,D}$ |

PBS: phosphate buffered saline; SBF: simulated body fluid; S: solubility. The mean with different lowercase letters in the same column indicate significant differences for films produced with starches prepared by different routes. Mean with different capital letters in the same column indicate significant differences between films prepared by the same route, but with the addition of the extract, as revealed by Tukey's test, $p \leq 0.05$.

is known that the TS values are related to the strength of the bonds between the molecules that compose the film.[84] If the film production occurs with pure starch only, it will have brittle characteristics and low mechanical resistance. The addition of plasticizers increases the mobility of the polymer chain, resulting in greater flexibility, extensibility, and ductility.[81] Plasticizers with OH groups are more interesting for this purpose, so glycerol was employed in this work. TS values between 9 and 29 MPa were obtained (Figure 8a). While evaluating the results, it was observed that AT and NT varied significantly within the group of precursor films.

Moreover, after incorporation, the significant variations were for BT-AB and NT-AB films within the group of films. Comparing the two groups, significant variation was observed for the BT/BT-AB pair. It was also noticed that, although the values tend to increase in the matrices with extract (BM-AB, BT-AB, and NT-AB), curiously, the NT-AB film, when compared to the precursors (NT), did not show significant variation. An increase of TS in the extract containing films is closely related to the extract's interactions with the polymeric chains of the film, as previously commented, adding a plasticizer increases the polymeric mobility. In this case, the extract would also help in this regard by improving the tensile strength of the film.

Devi and Dutta[81] reported that the increase in the tensile strength of the starch composites developed by them was related to hydrogen interactions between the polymer and the incorporated substance, which can justify the results, meaning that in the matrices with extract, the molecules are better organized and more strongly bonded.

While analyzing the E, Figure 8c, a very similar behavior with the TS values is noted. The extract incorporated films present higher E values than the precursors, and there was no significant variation within the group. An increase in the E values means greater rigidity in the material, and, therefore, less flexible, or stretchable they will be and greater will be the force necessary to break them. Thus, the values of E found for the matrices with extract are consistent with the hypothesis raised earlier, that the extract-matrix

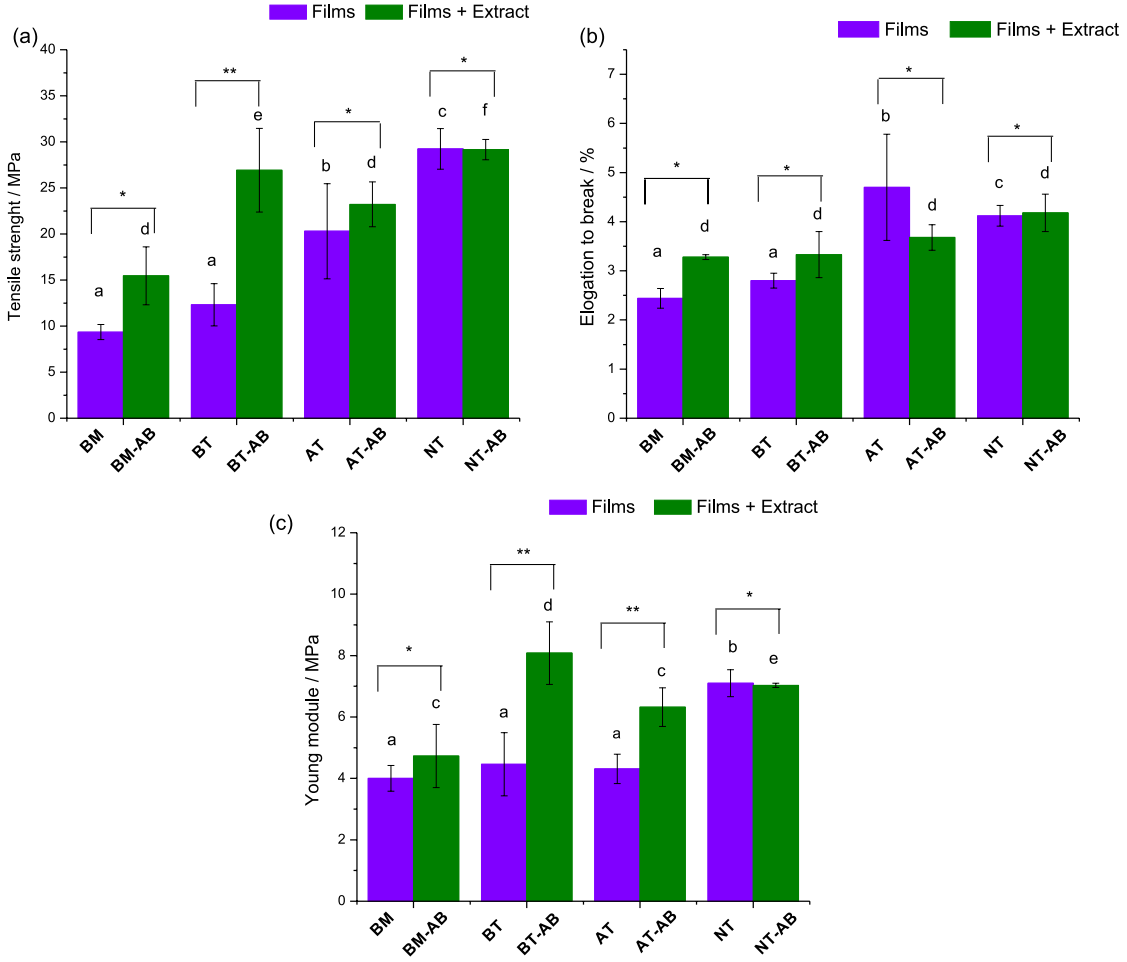


**Figure 8.** Mechanical properties of films (a) tensile at break (b) elongation at break, ε, and (c) Young's modulus, E. Statistical analysis was performed by evaluating the films in each test. Equal letters in equal colors indicate no statistically significant difference ($p \leq 0.05$) by Tukey's test. (*) Indicates no significant difference between a pair of samples, (**) indicates a significant difference between a pair of samples.

interaction occurs by stronger bonds, influencing the mechanical parameters of the material.

Moreover, it is also observed that for the values of elongation at break (ε), Figure 8b, within the group of precursor films, NT varied significantly, and within the group of films after incorporation of extract, the variations were significant for BT-AB and NT-AB. As for the pairs, BT/BT-AB and AT/AT-AB varied significantly. These data indicate that the presence of the extract makes the material more rigid, more resistant, and less flexible and that the different routes of obtaining starch influence the results.

Films destined for topical use should be preferably strong and flexible. In this work, we observed that the flexibility of the films was low. Although, this fact can be improved by swelling the matrices before application. A similar result was found by Shah *et al.*[77] when investigating the effect of green tea extract in wheat starch-sodium alginate films for wound healing, where the presence of the extract made the films more resistant and less flexible, due to the interactions between extract and the polymeric network.

### *In vitro* release assay

Figure 9 shows the *in vitro* release profiles of the AB extract. The BM-AB material showed a gradual release from the beginning until 20 h after the experiment, with a tendency to constant release from this time interval. This event can be justified by the fact that the babassu mesocarp *in natura* presents in its composition several other substances besides the major component (starch), which may suggest that in this case, the extract is weakly linked between the starch chains, causing its release in the first hours of contact with the extracting solution.

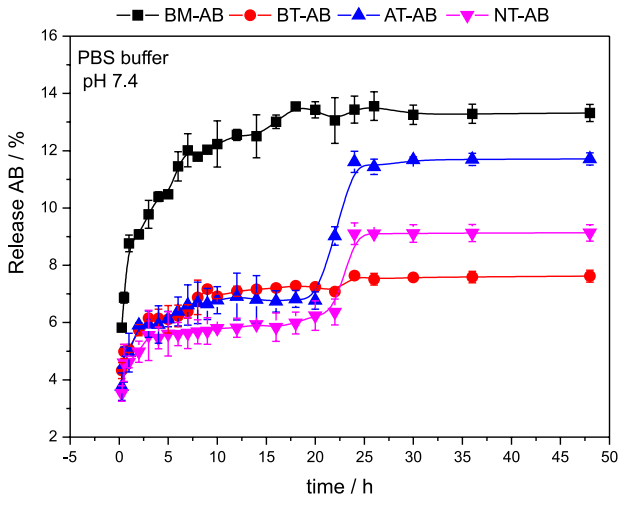


**Figure 9.** *In vitro* release profiles of AB extract from BM-AB (■), BT-AB (●), AT-AB (▲), and NT-AB (▼) matrices were performed in phosphate-buffered saline pH 7.4, for 48 h.

Different behavior was observed for BT-AB, AT-AB, and NT-AB materials, their first plateau was obtained within the first hour of the experiment, and the release occurred steadily for 20 h in all three cases, with the BT-AB film remaining with the same release rate until the end of the experiment. The AT-AB and NT-AB matrices, on the other hand, presented a new release stage with a new tendency to a plateau after 24 h. One hypothesis that could justify the observed fact is that the diffusion of the AB extract was facilitated as its initial concentration decreased, a behavior typical of polymeric systems whose release is mainly controlled by diffusion.

It was also observed that after 24 h, the AT-AB film presents a release rate of 11%, a little higher when compared to the NT-AB film, which was 9%. This can be explained by the mechanical behavior of these matrices, where the NT-AB film presented higher TS values than the AT-AB film, meaning that the latter is more resistant and, consequently, in it, the erosion is less pronounced.[85] In this instance, the diffusion process of the extract through the polymer matrix is slower, causing it to have a slightly lower release rate than the AT-AB film. These characteristics are important because they grant great versatility to the material.

According to the Korsmeyer-Peppas equation, a more thorough analysis was performed by applying mathematical modeling to the release profiles (equation 8). This model is suitable for drug release profiles with $M_t/M_\infty < 0.6$, for which the effects of polymer matrix erosion can still be neglected.[64] The fit provided good coefficients of determination ($R^2 \geq 0.901$). The calculated parameters and correlation coefficients are shown in Table 3. It can be noted that the n parameter was below 0.5 for all formulations, which indicates a *quasi*-Fickian transport[64] of the extract through the films. In other words, the release mechanism was determined by diffusion, as previously discussed. Furthermore, the n values obtained were close for all matrices, suggesting that the release mechanism was independent of the treatments employed in the starch extraction. These results may indicate that the extract was adsorbed to the polysaccharides by different types of interaction.

The k parameter was higher for the BM-AB film, indicating a faster release when compared to BT-AB, AT-AB, and NT-AB films. A possible explanation for this behavior is that the diffusion of the AB extract was facilitated when its initial concentration was lower, which is a characteristic of monolithic systems of drug release.[86] The therapeutic agent is dispersed in a polymeric matrix in this system, and the release rate depends on the initial concentration. If the concentration in the matrix is below the solubility limit, the system is controlled by diffusion. On

the other hand, if the concentration of the active ingredient is higher than its solubility limit in the matrix, the system is controlled by the dissolution of the active ingredient.[86] Thus, BT-AB, AT-AB, and NT-AB films were probably above the solubility limit in the tested system, being, therefore, less able to readily release the extract, working more efficiently for sustained release. Another explanation is that the extract may be more strongly adsorbed to the matrix, delaying the release.

**Table 3.** Kinetic parameter values for the Korsmeyer-Peppas model fitted to *in vitro* release data of AB extract collected for 48 h

| Sample | Korsmeyer-Peppas parameters | | |
|---|---|---|---|
| | k | n | $R^2$ |
| BM-AB | 0.2163 | 0.1475 | 0.9888 |
| BT-AB | 0.1384 | 0.0967 | 0.9850 |
| AT-AB | 0.1330 | 0.2658 | 0.9108 |
| NT-AB | 0.1354 | 0.1794 | 0.9018 |

k: rate constant; n: release exponent; $R^2$: coefficient of determination.

## Conclusions

The purification routes of babassu mesocarp were efficient, leading to materials with characteristic bands of amylaceous compounds (FTIR), C-type starch diffraction patterns, and homogeneous morphology (SEM). The films were efficiently produced by the conventional casting method, and it was possible to incorporate a complex matrix (AB extract) and study their release profile. The extract-matrix interaction was confirmed by the intensification of bands characteristic of the AB extract (FTIR) in the films and the definition of their diffraction profiles (XRD). The extract's incorporation into the matrix significantly changed its functional properties, such as humidity, fluid absorption, solubility, and mechanical properties. The *in vitro* release of the extract demonstrated that the system is controlled by diffusion due to the fitting to the Korsmeyer-Peppas model. Comparing the matrices with an incorporated extract of the untreated BM, it was noted that the chosen routes produced films with slower release behavior, meaning that the treatments employed in the starch purification are essential to improve the film's characteristics.

The results obtained in this work are promising and may represent an exciting starting point for the development of a new film formulation from babassu mesocarp for topical administration of the AB extract. Further *in vitro* and *in vivo* studies are required to confirm the appropriate application. Thus, from the considerations above, it can be inferred that the matrices can be employed to develop controlled release systems of plant extracts.

## Acknowledgments

The authors are grateful to FAPEMA for the financial support (UNIVERSAL-00877/18), to the Federal University of Maranhão, to the Analytical Center and CEMAT-UFMA for the analyses performed, to Prof Denilson Moreira Santos (DEDET-UFMA), for performing the mechanical tests on the films, to Prof Francisco Moura (UFMG) for the micrography analyses. LMC tanks CAPES for her master's degree fellowship.

### Author Contributions

Liane Miranda Carvalho was responsible for conceptualization, investigation, data curation, methodology, visualization, writing-original draft, review and editing; Luna Nascimento Vasconcelos for investigation; writing-review and editing; Letícia Nascimento de Oliveira for investigation, writing-review and editing, Cícero Wellington Brito Bezerra for conceptualization, funding acquisition, resources, writing-review and editing, project administration. Claudia Quintino da Rocha for conceptualization, methodology, supervision, writing - review and editing; Sirlane Aparecida Abreu Santana for conceptualization, methodology, supervision, funding acquisition, resources, writing - original draft, writing - review and editing, project administration.

## References

1. Semwal, R.; Joshi, S. K.; Semwal, R. B.; Semwal, D. K.; *Phytochem. Lett*. **2021**, *46*, 119. [Crossref]
2. Zhou, L.; Cai, L.; Ruan, H.; Zhang, L.; Wang, J.; Jiang, H.; Wu, Y.; Feng, S.; Chen, J.; *Int. J. Biol. Macromol.* **2021**, *183*, 1145. [Crossref]
3. Asfour, M. H.; Elmotasem, H.; Mostafa, D. M.; Salama, A. A. A.; *Int. J. Pharm*. **2017**, *534*, 325. [Crossref]
4. Paudel, K. R.; Wadhwa, R.; Tew, X. N.; Lau, N. J. X.; Madheswaran, T.; Panneerselvam, J.; Zeeshan, F.; Kumar, P.; Grupta, G.; Anand, K.; Singh, S. K.; Jha, N. K.; MacLoughlin, R.; Hansbro, N. G.; Lui, G.; Shukla, S. D.; Mehta, M.; Hansbro, P. M.; Dua, K.; *Life Sci*. **2020**, *276*, 119436. [Crossref]
5. Almeida, J. S.; Benvegnú, D. M.; Boufleur, N.; Reckziegel, P.; Barcelos, R. C. S.; Coradini, K.; Carvalho, L. M.; Bürger, M. E.; Beck, R. C. R.; *Drug Dev. Ind. Pharm*. **2012**, *38*, 792. [Crossref]
6. Tian, C.; Shao, Y.; Jin, Z.; Liang, Y.; Li, C.; Qu, C.; Sun, S.; Cui, C.; Lui, M.; *J. Pharm. Biomed. Anal*. **2022**, *209*, 114480. [Crossref]
7. Pandey, P.; Rahaman, M.; Bhatt, P. C.; Beg, S.; Paul, B.; Hafezz, A.; Al-Abbasi, F. A.; Nadeem, M. S.; Baothman, F. A.; Kumar, V.; *Nanomed. J*. **2018**, *13*, 8. [Crossref]

8. Resende, F. A.; Nogueira, C. H.; Espanha, L. G.; Boldrin, P. K.; Oliveira-Hohne, A. P.; de Camargo, M. S.; da Rocha, C. Q.; Vilegas, W.; Varanda, E. A.; *Regul. Toxicol. Pharmacol*. **2017**, *90*, 29. [Crossref]
9. Alcerito, T.; Barbo, F. E.; Negri, G.; Santos, D. Y. A. C.; Meda, C. I.; Young, M. C. M.; Chávez, D.; Blatt, C. T. T.; *Biochem. Syst. Ecol*. **2002**, *30,* 677. [Crossref]
10. Rocha, V. P. C.; da Rocha, C. Q.; Queiroz, E. F.; Marcourt, L.; Vilegas, W.; Grimaldi, B. G.; Furrer, P.; Allémann, E.; Wolfender, J.-L.; Soares, M. B. P.; *Molecules* **2019**, *24*, 1. [Crossref]
11. da Rocha, C. Q.; Vilela, F. C.; Cavalcante, G. P.; Santa-Cecília, F. V.; Santos-e-Silva, L.; dos Santos, M. H.; Giusti-Paiva, A.; *J. Ethnopharmacol*. **2011**, *133*, 396. [Crossref]
12. da Rocha, C. Q.; Queiroz, E. F.; Meira, C. S.; Moreira, D. R. M.; Soares, M. B. P.; Marcourt, L.; Vilegas, W.; Wolfender, J.-L.; *J. Nat. Prod*. **2014**, *77*, 1345. [Crossref]
13. da Rocha, C. Q.; Faria, F. M.; Marcourt, L.; Ebrahimi, S. N.; Kitano, B. T.; Ghirlardi, A, F.; Ferreira, A. L.; Almeida, A. C. A.; Dunder, R. J.; Souza-Brito, A. R. M.; Hamburger, M.; Vilegas, W.; Queiroz, E. F.; Wolfender, J-L.; *Phytochemistry* **2017**, *135*, 93. [Crossref]
14. Klein, T.; Longhini, R.; Bruschi, M. L.; Mello, J. C. P.; *Rev. Cienc. Farm. Basica Apl.* **2009**, *30*, 241. [Crossref]
15. Süntar, I.; *Phytochem. Rev*. **2019**, *19*, 1199. [Crossref]
16. Hasan, T.; Jahan, E.; Ahmed, K. S.; Hossain, H.; Siam, S. M. M.; Nahid, N.; Mazumder, T.; Shuvo, M. S. R.; Daula, A. F. M. S. U.; *Biomed. Pharmacother*. **2022**, *148*, 112774. [Crossref]
17. Costa, N. N.; Lopes, L. F.; Ferreira, D. F.; de Prado, E. M. L.; Saveri, J. A.; Resende, J. A.; Careta, F. P.; Ferreira, M. C. P.; Carreira, L. G.; Souza, S. O. L.; Cotrim, M. A. P.; Boeing, T.; Andrade, S. F.; Oréfice, R. L.; Villanova, J. C. O.; *Mater. Sci. Eng. C* **2020**, *109*, 110643. [Crossref]
18. Shedoeva, A.; Leavesley, D.; Upton, Z.; Fan, C.; *J. Evidence-Based Complementary Altern. Med.* **2019**, 2684108. [Crossref]
19. Korde, B. A.; Mankar, J. S.; Phule, S.; Krupadam, R. J.; *Mater. Sci. Eng. C* **2019**, *99*, 222. [Crossref]
20. Ghorpade, V. S.; Dias, R. J.; Mali, K. K.; Mulla, S. I.; *J. Drug Delivery Sci. Technol.* **2019**, *52*, 421. [Crossref]
21. Abureesh, M. A.; Oladipo, A. A.; Mizwari, Z. M.; Berksel, E.; *Int. J. Biol. Macromol*. **2018**, *116*, 417. [Crossref]
22. Leal, A. S.; de Araújo, R.; Souza, G. R.; Lopes, G. L. N.; Pereira, S. T.; Alves, M. M. M.; Barreto, H. M.; Carvalho, A. L. M.; Ferreira, P. M. P.; Silva, D.; Carvalho, F. A. A.; Lopes, J. A. D.; Nunes, L. C. C.; *Carbohydr. Polym*. **2018**, *201*, 113. [Crossref]
23. Marín, T.; Montoya, P.; Arnache, O.; Pinal, R.; Calderón, J.; *Mater. Des*. **2018**, *152*, 78. [Crossref]
24. Gajendiran, M.; Jo, H.; Kim, K.; Balasubramanian, S.; *J. Ind. Eng. Chem*. **2019**, *77*, 181. [Crossref]
25. Boehler, C.; Oberueber, F.; Asplund, M.; *J. Controlled Release* **2019**, *304,* 173. [Crossref]
26. Basu, T.; Pal, B.; Singh, S.; *Particuology* **2018**, *40*, 169. [Crossref]
27. Tsai, Y.-H.; Yang, Y.-N.; Ho, Y.-C.; Tsai, M.-L.; Mi, F.-L.; *Carbohydr. Polym*. **2018**, *180*, 286. [Crossref]
28. Chin, S. F.; Jimmy, F. B.; Pang, S. C.; *J. Drug. Delivery Sci. Technol*. **2018**, *43*, 262. [Crossref]
29. Luo, C.; Yang, Q.; Lin, X.; Qi, C.; Li, G.; *Int. J. Biol. Macromol*. **2019**, *125*, 721. [Crossref]
30. Taghizadeh, M. T.; Ashassi-Sorkhabi, H.; Afkari, R.; Kazempour, A.; *Int. J. Biol. Macromol*. **2019**, *131*, 581. [Crossref]
31. Bonilla, P.; Arias, E. M.; Solans, C.; García-Celma, M. J.; *Colloids Surf., A* **2018**, *536*, 148. [Crossref]
32. Freitas, E. D.; Vidart, J. M.; Silva, E. A.; da Silva, M. G. C.; Vieira, M. G. A.; *Particuology* **2018**, *41*, 65. [Crossref]
33. Rocha-García, D.; de Lourdes Betancourt-Mendiola, M.; Wong-Arce, A.; Rosales-Mendoza, S.; Reyes-Hernández, J.; González-Ortega, O.; Palestino, G.; *Eur. Polym. J*. **2018**, *108*, 485. [Crossref]
34. Pal, A.; Bajpai, J.; Bajpai, A. K.; *J. Drug Delivery Sci. Technol*. **2018**, *45*, 323. [Crossref]
35. Thauvin, C.; Schwarz, B.; Delie, F.; Allémann, E.; *Int. J. Pharm*. **2018**, *548*, 771. [Crossref]
36. Zheng, W.; Li, M.; Lin, Y.; Zhan, X.; *Biomed. Pharmacother*. **2018**, *108*, 565. [Crossref]
37. Wang, J.; Helder, L.; Shao, J.; Jansen, J. A.; Yang, M.; Yang, F.; *Int. J. Pharm*. **2019**, *564*, 1. [Crossref]
38. Evangeline, S.; Sidharan, T. B.; *Int. J. Biol. Macromol*. **2019**, *135*, 945. [Crossref]
39. Farrag, Y.; Ide, W.; Montero, B.; Rico, M.; Rodríguez-Llamazares, S.; Barral, L.; Bouza, R.; *Int. J. Biol. Macromol.* **2018**, *118*, 2201. [Crossref]
40. Quadrado, R. F. N.; Fajardo, A. R.; *Arabian J. Chem*. **2018**, *13*, 2183. [Crossref]
41. Chan, S. Y.; Goh, C. F.; Lau, J. Y.; Tiew, Y. C.; Balakrishnan, T.; *Int. J. Pharmacol*. **2019**, *562*, 203. [Crossref]
42. Oshiro Jr., J. A.; Shiota, L. M.; Chiavacci, L. A.; *Matéria* **2014**, *10*, 24. [Crossref]
43. Dong, S.; Li, S.; Hao, Y.; Gao, Q.; *Int. J. Biol. Macromol*. **2019**, *134*, 165. [Crossref]
44. Maniglia, B. C.; Tessaro, L.; Lucas, A. A.; Tapia-Blácido, D. R.; *Food Hydrocoll*. **2017**, *70*, 383. [Crossref]
45. Maniglia, B. C.; Tapia-Blácido, D. R.; *Food Hydrocoll*. **2016**, *55*, 47. [Crossref]
46. Suh, J. H.; Ock, S. Y.; Park, G. D.; Lee, M. H.; Park, H. J.; *Polym. Test*. **2020**, *89*, 106612. [Crossref]
47. Li, C.; Hu, Y.; *LWT-Food Sci. Technol*. **2021**, *148*, 111942. [Crossref]
48. Wu, Z.; Qiao, D.; Zhao, S.; Lin, Q.; Zhang, B.; Xie, F.; *Int. J. Biol. Macromol*. **2022**, *203*, 153. [Crossref]

49. Bisharat, L.; Barker, S. A.; Narbad, A.; Craig, D. Q.; *Int. J. Pharm*. **2019**, *556*, 311. [Crossref]
50. do Evangelho, J. A.; Dannenberg, G. S.; Biduski, B.; el Halal, S. L. M.; Kringel, D. H.; Gularte, M. A.; Fiorentimi, A. M.; Zavareze, E. R.; *Carbohydr. Polym*. **2019**, *222*, 114981. [Crossref]
51. Muller, J.; Quesada, A. C.; González-Martínez, C.; Chiralt, A.; *Eur. Polym. J.* **2017**, *96*, 316. [Crossref]
52. Nieto-Suaza, L.; Acevedo-Guevara, L.; Sánchez, L. T.; Pinzón, M. I.; Villa, C. C.; *Food Struct*. **2019**, *22*, 100131. [Crossref]
53. Amorim, E.; Matias, J. E. F.; Coelho, J. C. U.; Campos, A. C. L.; Stahlke Jr., H. J.; Timi, J. R. R.; Rocha, L. C. A.; Moreira, A. T. R.; Rispoli, D. Z.; Ferreira, L. M.; *Acta Cir. Bras*. **2006**, *21*, 67. [Crossref]
54. Azevedo, A. P. S.; Farias, J. C.; Costa, G. C.; Ferreira, S. C. P.; Aragão-Filho, W. C.; Sousa, P. R. A.; Pinheiro, M. T.; Maciel, M. C. G.; Silva, L. A.; Lopes, A. S.; Barroquerio, E. S. B.; Borges, M. O. R.; Guerra, R. N. M.; Nascimento, F. R. F.; *J. Ethnopharmacol.* **2007**, *111*, 155. [Crossref]
55. Nobre, C. B.; de Sousa, E. O.; de Lima Silva, J. M. F.; Coutinho, H. D. M.; da Costa, J. G. M.; *Eur. J. Integr. Med*. **2018**, *23*, 84. [Crossref]
56. Pellenz, N. L.; Barbisan, F.; Azzolin, V. F.; Marques, L. P. S.; Mastella, M. H.; Teixeira, C. F.; Ribeiro, E. E.; da Cruz, I. B. M.; *Wound Med*. **2019**, *26*, 100163. [Crossref]
57. Rodrigues, S. C. S.; da Silva, A. S.; de Carvalho, L. H.; Alves, T. S.; Barbosa, R.; *J. Mater. Res. Technol*. **2020**, *9*, 15670. [Crossref]
58. Mukurumbira, A. R.; Mellem, J. J.; Amonsou, E. O.; *Carbohydr. Polym*. **2017**, *165*, 142. [Crossref]
59. Moreno, O.; Cárdenas, J.; Atarés, L.; Chiralt, A.; *Carbohydr. Polym*. **2017**, *78*, 147. [Crossref]
60. Association of Official Analytical Chemists (AOAC); *Official Methods of Analysis: 930.04*, AOAC: Washington, DC, USA, 2004.
61. Kokubo, T.; Kushitani, H.; Sakka, S.; Kitsugi, T.; Yamamuro, T.; *J. Biomed. Mater. Res* **1990**, *24*, 721. [Crossref]
62. ASTM D882-18: *Standard Test Method for Tensile Properties of Thin Plastic Sheeting*, West Conshohocken, 2012.
63. Bueno, C. Z.; Moraes, A. M.; *Mater. Sci. Eng., C* **2018**, *93*, 671. [Crossref]
64. Altunkaynak, F.; Okur, M.; Saracoglu, N.; *J. Drug Delivery Sci. Technol*. **2022**, *68*, 103099. [Crossref]
65. Andrade, L. B. S.; Julião, M. S. S.; Cruz, R. C. V.; Rodrigues, T. H. S.; Fontenelle, R. O. S.; da Silva, A. L. C.; *Ind. Crops Prod*. **2018**, *125*, 220. [Crossref]
66. Vieira, A. P.; Santana, S. A. A.; Bezerra, C. W. B.; Silva, H. A.; de Melo, J. C. P.; da Silva Filho, E. C.; Airoldi, C.; *Chem. Eng. J.* **2010**, *161*, 99. [Crossref]
67. Vieira, A. P.; Santana, S. A. A.; Bezerra, C. W. B.; Silva, H. A.; Chaves, J. A. P.; de Melo, J. C.; da Silva Filho, E. C.; Airoldi, C.; *J. Hazard. Mater*. **2009**, *166*, 1272. [Crossref]
68. do Nascimento, J. M.; de Oliveira, J. D.; Leite, S. G. F.; *Environ. Technol. Innovation* **2019**, *16*, 100440. [Crossref]
69. Lin, L.; Guo, D.; Zhao, L.; Zhang, X.; Wang, J.; Zhang, F.; Wei, C.; *Food Hydrocolloids* **2016**, *52*, 19. [Crossref]
70. Denardin, C. C.; da Silva, L. P.; *Cienc. Rural*. **2009**, *39*, 945. [Crossref]
71. Zhai, Y.; Li, X.; Bai, Y.; Jin, Z.; Svensson, B.; *Food Hydrocolloids* **2022**, *124*, 107256. [Crossref]
72. Monteiro, F. S.; Costa, J. R. S.; Martins, L. J. A.; da Rocha, C. Q.; Borges, A. C. R.; Rocha Borges, M.; O.; *J. Basic Appl. Pharm. Sci.* **2020**, *41*, e667. [Crossref]
73. da Rocha, C. Q. D.; Vilela, F. C.; Santa-Cecília, F. V.; Cavalcante, G. P.; Vilegas, W.; Giusti-Paiva, A.; dos Santos, M. H. D.; *Rev. Bras. Farmacogn*. **2015**, *25*, 228. [Crossref]
74. de Matos, Y. M.; Vasconcelos, D. L.; Barreto, A. C.; Rocha, J. E.; Neto, J. B.; Campina, F. F.; Guedes, T. T. A. M.; Sousa, A. K.; Teixeira, R. N. P.; Alvarez-Pizarro, J. C.; Coutinho, H. D. M.; da Silva, J. H.; *Vib. Spectrosc*. **2020**, *109*, 103084. [Crossref]
75. Hooresfand, Z.; Ghanbarzadeh, S.; Hamishehkar, H.; *Pharm. Sci*. **2015**, *21*, 145. [Crossref]
76. Henning, F. G.; Ito, V. C.; Demiate, I. M.; Lacerda, L. G.; *Carbohydr. Polym. Technol. Appl*. **2022**, *4*, 100157. [Crossref]
77. Shah, Z.; Fernandes, C.; Suares, D.; *J. Drug Delivery Sci. Technol*. **2019**, *52*, 255. [Crossref]
78. Mali, S.; Grossmann, M. V. E.; Yamashita, F.; *Semina: Cienc. Agrar*. **2010**, *31*, 137. [Crossref]
79. Batool, S.; Hussain, Z.; Niazi, M. B. K.; Liaqat, U.; Afzal, M.; *J. Drug Delivery Sci. Technol*. **2019**, *52*, 403. [Crossref]
80. Ahmed, A.; Niazi, M. B. K.; Jahan, Z.; Ahmad, T.; Hussain, A.; Pervaiz, E.; Janjua, H. A.; Hussain, Z.; *Eur. Polym. J*. **2020**, *130*, 109650. [Crossref]
81. Devi, N.; Dutta, J.; *Int. J. Biol. Macromol*. **2019**, *127*, 222. [Crossref]
82. Bueno, C. Z.; Dias, A. M. A.; Sousa, H. J. C.; Braga, M. E. M.; Moraes, A. M.; *Mater. Sci. Eng., C* **2014**, *44*, 117. [Crossref]
83. Waghmare, V. S.; Wadke, P. R.; Dyawanapelly, S.; Deshpande, A.; Jain, R.; Dandekar, P.; *Bioact. Mater*. **2018**, *3*, 255. [Crossref]
84. Nizam, N. H. M.; Rawi, N. F. M.; Ramle, S. F. M.; Abd Aziz, A.; Abdullah, C. K.; Rashedi, A.; Kassim, M. H. M.; *J. Mater. Res. Technol.* **2021**, *15*, 1572. [Crossref]
85. Chen, J.; Li, X.; Chen, L.; Xie, F.; *Carbohydr. Polym*. **2019**, *191*, 242. [Crossref]
86. Raval, A.; Parikh, J.; Engineer, C.; *Braz. J. Chem. Eng*. **2010**, *27*, 211. [Crossref]


*Submitted: November 17, 2022*
*Published online: March 30, 2023*